2024 IEEE 63rd Conference on Decision and Control (CDC)
December 16-19, 2024. MiCo, Milan, Italy

A Novel Hamiltonian Approach for Modeling and Control of Quasi-Resonant Buck Converters*

Agustín Sánchez-Contreras[1], Isaac Ortega-Velázquez[1], Oscar Rodríguez-Benítez[1] and Gerardo Espinosa-Pérez[1]

Abstract— **In this paper are presented a novel modeling approach and a passivity-based control scheme to solve the output voltage regulation control problem of a class of Quasi-resonant Converters. Instead of consider classical order reduction arguments, the proposed full order model recovers the Port-Controlled Hamiltonian structure naturally exhibited by the converters. This feature leads to the possibility to propose the implementation of a passive PI control scheme which has been widely recognized to achieve high performances while proving in a formal way its stability properties. In addition, the controller structure is complemented by the inclusion of a static map to use both the frequency and the duty-cycle of the square input signal as control input, guaranteeing a Zero Current Switching operation mode which drastically improves the efficiency of the circuit. The usefulness of the proposed model and control are validated in a numerical setting.**

I. INTRODUCTION

Electric energy management has experienced drastic changes due to the appearance of new concerns like climate change and sustainable development. In this context power electronics plays a fundamental role owing to its capacity to process electric energy with high efficiency and low cost while taking into account technical and economic aspects.

In spite of the fact that power converters can be used in a vast number of applications, a common challenge refers to achieve a proper operation with a reduced number of components, reducing conduction losses and featuring low-voltage stress on the semiconductors. Thus, the introduction of high-frequency-link power conversion systems has emerged as a viable alternative to eliminate the use of bulky, heavy, lossy, and noisy equipment. Moreover, resonant converters establish a frequently implemented topology specially for modern applications [1].

Resonant topologies achieve high power density, reduced weight, and low noise without compromising efficiency, cost, and reliability. These features come from the introduction of inductors and capacitors as part of resonance circuits and achieving Zero-Voltage Switching (ZVS) or Zero-Current Switching (ZCS) operation modes, known as soft-switching operation.

Resonant topologies has received a lot of attention from the power electronics community and state a research topic of current interest [2], [3], [4]. However, it is difficult to find the proposition and analysis of model-based (nonlinear) control schemes derived from the control theory community. One reason that explains this situation is that dynamical models for this kind of converters are highly nonlinear steering the efforts to the use of simplified approximations [5], [6], [7], [8].

With the aim to reduce the gap between applied and theoretical results for the control of resonant converters, in this paper both the modeling and control design for one kind of these systems are approached from a novel perspective. The main characteristic of the contribution lies in the fact that instead of trying to simplify the model of the converters, the Hamiltonian structure [9] naturally exhibited by them is recovered leading to the possibility to propose control schemes from the nonlinear control theory that has shown to be very effective to solve the stabilization problem guaranteeing high performance operation. In particular, in this paper the well-known Passivity-based Control (PBC) methodology design is considered [9], [10], [11].

Although the results presented in this contribution can be extended to several resonant topologies, with the aim to present them in a clear way the particular class of resonant circuits considered in this paper is the DC-DC Quasi-resonant Buck converters (QRBC). This kind of circuits is widely implemented as voltage regulation modules to provide energy to a DC distribution system or conditioning the voltage as an intermediate stage of a DC–AC conversion system, for example in electric vehicles chargers [12], [13] or to fed light emitting diode (LED) loads [14], among other.

The importance of QRBC has been well recognized since several years ago [15]. However, from the control point of view, the proposition of novel control strategies is very limited concentrating the efforts to the use of classical PI schemes [16], [17]. One of the principal reasons that has limited the development of model-based control laws is the complexity of the current mathematical model reported in the literature, known as Generalized State-Space Averaging (GSSA) model [18]. This approach, in addition to the aforementioned analysis problems, has led to the usual practice of consider the use of fixed duty-cycle for the control input which induces to the lost of soft-switching operation, the essence of this kind of topologies.

On the other hand, PBC has provided solutions to control problems related with power electronics exhibiting both formally proved strong stability properties and high dynamical performances. Actually, some topologies of resonant converters, including QRBC, have been approached from the passivity perspective [19], [20], [21]. Unfortunately, the advantages offered by the PBC methodology design are

*Part of the work of G. Espinosa-Pérez was supported by DGAPA-UNAM under the grant IN109622. The work of O. Rodríguez was supported by DGAPA-UNAM under the Programa de Becas Posdoctorales de la UNAM.

[1]Universidad Nacional Autónoma de México, Facultad de Ingeniería-UNAM, México. gerardoe@unam.mx

only partially exploited since simplified models, basically the GSSA model, are considered.

In this paper the output voltage regulation control problem of QRBC is solved. The main features of the contribution are:

- It is developed a complete Port-Controlled Hamiltonian (PCH) representation without omitting the states that correspond to the resonant sub-circuit. Up to the best of the authors knowledge, this is the first time that this model is reported in the literature.
- Based on the PCH representation of the system, a passive Proportional-Integral (PI) controller is introduced following ideas of [11] but solving the desired trajectories definition step from an efficiency perspective.
- In order to formally prove the stability properties of the proposed control scheme, the input square signal of the circuit is expressed in terms of its Taylor series representation leading to the possibility to consider as control inputs both the duty-cycle and the frequency of this signal.
- A recently reported result [22] is considered to compute, in terms of the current demanded by the load and the frequency, the duty-cycle that guarantees ZCS operation.

The rest of the paper is organized as follows: In Section II the operation of the QRBC and the proposed model are presented together with the module that allows the use of varying duty-cycle. The development of the PBC is included in Section III while the numerical evaluation of both the proposed model and the control scheme is carried out in Section IV. Some concluding remarks are included in Section V.

II. Hamiltonian modeling of QRBC

In this section one of the main contributions of the paper is presented, namely, a novel approach for modeling a QRBC which is based on identifying the natural PCH structure exhibited by this circuit.

In Figure 1 is presented the considered topology of a QRBC. It is composed by a voltage source V_g, a switch S_1, a resonant tank made up of L_r and C_r, a diode D_0 and an output L_0, C_0 filter. For the sake of clarity of presentation, it is considered a linear load represented by R.

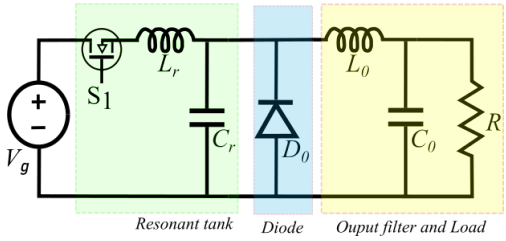

Fig. 1. Quasi-Resonant Buck Converter

The operation of the converter has been clearly described since several years ago [18]. The purpose of the switching elements S_1, D_0 is to shape both current and voltage of the tank L_r, C_r into a quasi-sinusoidal signal with frequency near the resonant frequency looking the output filter as a constant current sink. This operation offers the advantage that commutation can be carried out when the resonant current crosses zero reducing drastically the switching losses and increasing the efficiency, leading also to a high density power operation.

From the usual modeling perspective, since the converter is designed considering that $L_0 >> L_r$, two types of dynamical states are identified: fast (resonant) states and slow (output filter) states. With this differentiation at hand, the four sets of differential equations obtained for the four operation stages that compose a full switching cycle can be reduced to a system of only two differential equations by explicitly solving those that correspond to the fast states and substituting these solutions into the equations that describe the behavior of the slow states. This procedure leads to the well-known and widely accepted GSSA model of the converter [18], [17], [8].

The apparent advantage of working with a reduced order model like the GSSA model, is contradicted by the complex structure of its input, in addition to the necessity to deal with a highly unstructured nonlinear system, the impossibility to identify the use of the duty cycle of the original square input signal which is fundamental to achieve ZCS operation.

Instead of looking for a reduced order representation, in this paper the purpose is to analyze the full order model but putting attention to is natural PCH structure in order to take advantage for a systematic design of a control law. In this sense, the modeling procedure is divided into three steps dedicated to obtain a dynamical representation of the resonant tank, the diode D_0 and the output filter.

Concerning the resonant tank, it can be obtained that its dynamic behavior is described by

$$\begin{aligned} L_r\dot{i}_r + \alpha_1 v_r &= \alpha_1 V_g \\ C_r\dot{v}_r - \alpha_1 i_r &= -i_1 \end{aligned} \tag{1}$$

where the value of signal α_1 belongs to the discrete set $\{0, 1\}$ to recover the operation when the switch S_1 is open and closed, respectively. In addition, i_r is the current across inductor L_r, v_c stands for the voltage at terminals of C_r, V_g is the voltage of the input source and i_1 is the output current of the tank that is fed to the diode D_0.

With respect the diode D_0, this device can be viewed as a power preserving connector with associated variables as described in Figure 2. Thus, it operation can be written as

$$\begin{bmatrix} v_d \\ i_1 \end{bmatrix} = \begin{bmatrix} 0 & -\alpha_2 \\ \alpha_2 & 0 \end{bmatrix} \begin{bmatrix} i_0 \\ v_r \end{bmatrix} \tag{2}$$

where i_0, v_d are the port variables at the side of the output filter, while the signal α_2 equals to 1 when $v_r > 0$ (reverse bias polarization) or takes the value 0 when $v_r \leq 0$ (forward bias polarization).

Regarding the output filter behavior, it is clear that it can be represented by

$$\begin{aligned} L_0\dot{i}_0 + v_0 &= v_d \\ C_0\dot{v}_0 - i_0 &= -i_l \end{aligned} \tag{3}$$

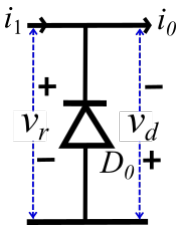

Fig. 2. Diode D_0 as power preserving connector

where i_0 is the current crossing inductor L_0, v_0 is the voltage at terminals of C_0, and i_l is the load current which takes the form $i_l = \frac{1}{R}v_0$ for the considered linear load.

In order to complete the analysis to obtain the proposed model, it is necessary to recall the relationship between current and voltage variables with the fundamental hamiltonian variables. This is done by noting that the flux linkage of the inductors is given $\lambda_r = L_r i_r$ and $\lambda_0 = L_0 i_0$ while the charge of the capacitors take the form $q_r = C_r v_r$ and $q_0 = C_0 v_0$.

Considering the dynamic behavior of the components of a QRBC, it is possible to formulate a PCH representation of the complete circuit. For this purpose, define as state variables $x_1 = \lambda_r$, $x_2 = q_r$, $x_3 = \lambda_0$ y $x_4 = q_0$. Under these conditions, the total storage energy function of the system takes the form

$$H(x) = \frac{1}{2}x^T P x \tag{4}$$

with

$$x = \begin{bmatrix} x_1 \\ x_2 \\ x_3 \\ x_4 \end{bmatrix} \quad P = \begin{bmatrix} \frac{1}{L_r} & 0 & 0 & 0 \\ 0 & \frac{1}{C_r} & 0 & 0 \\ 0 & 0 & \frac{1}{L_0} & 0 \\ 0 & 0 & 0 & \frac{1}{C_0} \end{bmatrix}$$

Hence, combining (1), (2) and (3), the complete dynamical model of the QRBC is given by

$$\dot{x} = J(\alpha_2)\nabla H(x) + G(x)\alpha_1 + \xi, \tag{5}$$

where

$$J(\alpha_2) = \begin{bmatrix} 0 & 0 & 0 & 0 \\ 0 & 0 & -\alpha_2 & 0 \\ 0 & \alpha_2 & 0 & -1 \\ 0 & 0 & 1 & 0 \end{bmatrix}$$

while $G(x) = J_1 \nabla H(x) + G_1$ with

$$J_1 = \begin{bmatrix} 0 & -1 & 0 & 0 \\ 1 & 0 & 0 & 0 \\ 0 & 0 & 0 & 0 \\ 0 & 0 & 0 & 0 \end{bmatrix}$$

and

$$G_1 = \begin{bmatrix} V_g \\ 0 \\ 0 \\ 0 \end{bmatrix}; \quad \xi = \begin{bmatrix} 0 \\ 0 \\ 0 \\ -i_l \end{bmatrix}$$

It must be noticed that model (5) exhibits the characteristic that signals α_1 and α_2 are discontinuous. While the latter does not impose a problem to carry out analysis and control design since it appears in the skew-symmetric interconnection matrix, the former requires a different treatment since it corresponds to the control input. This situation is approached in the next section.

A. Continuous approximation of control input α_1

With the aim to have a compatible input signal for model (5) that could be used for analysis and control design purposes, the effect of α_1 must be represented by a continuous signal. To do this, it is convenient to recognize that this signal, during a complete operation cycle, takes the form described in Figure 3.

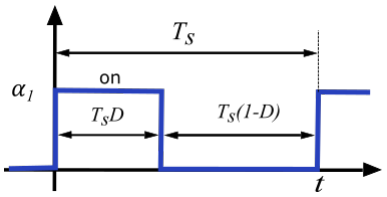

Fig. 3. Discontinuous control input α_1

It is clear that the shape of α_1 is determined by both the duty cycle D and the frequency $f_s = \frac{1}{T_s}$. The amplitude A could be also considered as a degree of freedom, but in practice this parameter is considered fixed. Indeed, both D and f_s constitute the control inputs in a practical setting since there exist integrated circuits whose function is the transformation of continuous values of these signals into a square signal like the described in Figure 3.

Under an operation cycle, f_s determines the operation frequency of the resonant tank while D must be adjusted depending on the value of the resonant current i_r in order to achieve ZCS. It is interesting to notice at this point that, due to the fact that in the GSSA model the effect of D is hidden, a common practice is to fix D leading to the impossibility to guarantee ZCS when load perturbations appear.

To obtain the desired continuous representation, consider that

$$\alpha_1(t) = \begin{cases} A & \text{if} \quad \delta \le t \le \delta + T_s D \\ 0 & \text{if} \quad \delta + T_s D < t < \delta + T_s \end{cases} \tag{6}$$

where $\delta \ge 0$ is the initial time of the cycle.

The idea followed in this paper is to consider the complex Fourier expansion of α_1 given by

$$\alpha_1(t) = \sum_{n=-\infty}^{\infty} C_n e^{jn\omega_s t} \tag{7}$$

where

$$C_n = \frac{1}{T_s}\int_{T_s} \alpha_1(t) e^{-jn\omega_s t} dt \tag{8}$$

Considering (6), it is obtained

$$C_n = \frac{1}{2j\pi n}\left(1 - e^{-2j\pi n D}\right) \tag{9}$$

where, without loss of generality, it has been considered $\delta = 0$, $A = 1$ and $\omega_s = \frac{2\pi}{T_s}$. Hence, expression (7) is written as

$$\alpha_1(t) = D + 2\sum_{n=1}^{\infty} \mathrm{Re}\left[C_n e^{jn\omega_s t}\right] \tag{10}$$

since the terms of order $-n$ correspond to the complex conjugate of the terms of order n.

The advantage of the representation (10) is that it clearly recovers the effect of both the duty cycle D and the frequency f_s. Of course, the approximation of the square signal α_1 will depend on how many terms n are considered.

B. Relationship between f_s and D.

In this section the problem of using the duty cycle D as a control input instead of consider it with a fixed value is approached. In this sense, a novel result reported in [22] is included in the modeling of the QRBC.

The aforementioned result refers to the establishment of a relationship between the resonant frequency f_s and the duty cycle D that guarantees that voltage regulation is achieved, even in presence of load variations, assuring at the same time that ZCS operation is not lost.

The result is based on the approximation of the behavior of the resonant current i_r during the time period when switch S_1 is closed, *i.e*, when $\alpha_1 = 1$. This behavior is shown in Figure 4 and corresponds to the described by (1).

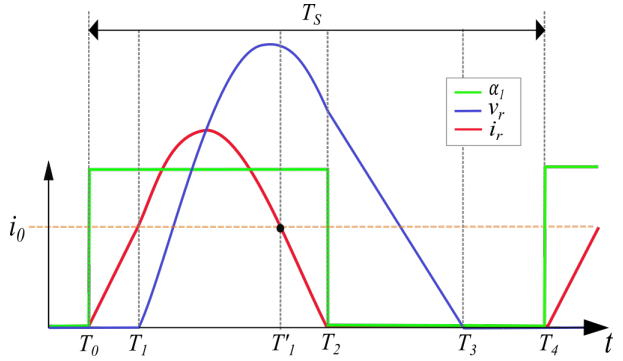

Fig. 4. Resonant variables behavior

It can be noticed that during the time period $T_1 - T_0$, the current i_r grows in a linear way satisfying

$$T_1 - T_0 = \frac{L_r}{V_g} i_0$$

On the other hand, for the time period $T_2 - T_1$ the current i_r and the voltage v_r evolve in a resonant way. In particular, from time T_1 to T'_1 this behavior is given by

$$\begin{aligned} v_r &= V_g\,(1 - \cos\omega_r t) \\ i_r &= i_o + \frac{V_g}{Z_r}\sin\omega_r t \end{aligned}$$

with $Z_r = \sqrt{\frac{L_r}{C_e}}$ and $\omega_r = \frac{1}{\sqrt{L_r C_r}}$. Hence, it holds that

$$T'_1 - T_1 = \pi\sqrt{L_r C_r}$$

Although during the time period $T_2 - T'_1$ the system still operates in resonant mode, it is possible to linearize the current behavior in such way that the following expression is obtained

$$T_2 - T'_1 = \frac{L_r}{V_g} i_0$$

From the results presented above and Figure 3, the duty cycle takes the form

$$D = f_s \left[\frac{2L_r}{V_g} i_0 + \pi\sqrt{L_r C_r}\right] \tag{11}$$

The importance of this equation lies in the fact that if D is computed in this way, then the switch S_1 will be opened when the current i_r crosses zero even when the frequency f_s varies.

C. Complete continuous model of QRBC

Once the practical operation of the approached converter has been taken into account, it is possible to formulate a dynamical model that satisfy the mathematical conditions necessary to carry out model-based analysis and control design.

In this sense, notice that from a mathematical perspective equation (10) and (11) can be viewed as a static map from the signal f_s to the variable $\alpha_1(D, f_s)$ which can be considered linear with respect f_s and that neither influence the stability properties nor modify the PCH structure of system (5). Actually, any closed-loop control system will take the structure depicted in Figure 5. Thus, for the rest of the paper it will be considered that the control input of system (5) is f_s for all practical purposes.

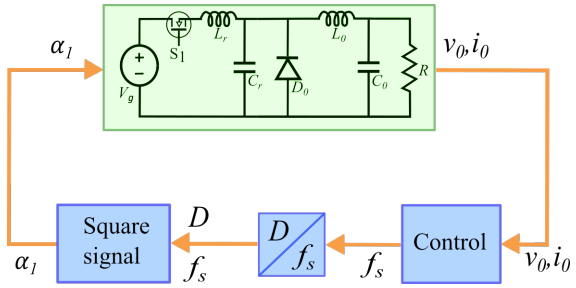

Fig. 5. Generic closed-loop system

III. Passivity-based Control of QRBC

In this section the second main result of the contribution is presented, namely, the formal proof that the use of passivity-based arguments can be used to solve the output voltage regulation control problem of QRBC. This part of the proposed results is based in well-known properties of the control of PCH systems. In particular, the passivity properties of model (5) are identified to later on propose the use of a passive PI control like the considered in [11].

In order to solve the considered control problem, it is first necessary to define what in the PBC literature is known as the admissible trajectories. This term corresponds to the achievable behavior of the controlled system, denoted as $x^\star$, and therefore these trajectories must be solution of the equations given by

$$\dot{x}^\star = J(\alpha_2)\nabla H(x^\star) + G(x^\star)\alpha_1(D^\star, f_s^\star) + \xi \tag{12}$$

On the other hand, it can be straightforwardly proved that the PCH system given by (5) defines a passive map of the form

$$\Sigma: \ \alpha_1(D, f_s) \to y$$

with $y = G_1^\top P x$.

As will be clear below, for the controller implementation it is necessary to compute from (12) the value of $f_s^\star$ that corresponds to a prescribed $x^\star$. This is done by noting that this system enjoys the same aforementioned passivity property that comes from the power balance

$$\dot{H}(x^\star) = -\frac{1}{C_0} x_4^\star i_l + (y^\star)^\top \alpha_1(D^\star, f_s^\star)$$

It is well-known [18] that the desired solution corresponds to the voltage conversion ratio of the converter that takes the next form

$$f_s^\star = \frac{v_0^\star}{V_g}\left(\frac{1}{T_3(i_0^\star) - \frac{T_1(i_0^\star)}{2}}\right) \tag{13}$$

where it is considered $T_0 = 0$. With these elements at hand, it is possible to formulate the next proposition where the considered control law is presented.

Proposition. *Consider the PCH model of the QRBC given by (5). Assume that a prescribed $x^\star$ is given that corresponds to the desired constant value for the output voltage of the converter. Under these conditions, the control law*

$$\begin{aligned} f_s &= -K_p y + K_I \zeta + f_s^\star \\ \dot{\zeta} &= -y \\ y &= G_1^\top P \tilde{x} \end{aligned} \tag{14}$$

with $f_s^\star$ as in (13), the error variable $\tilde{x} = x - x^\star$ and $K_p, K_I > 0$ guarantees that

$$\lim_{t\to\infty} x - x^\star = 0 \tag{15}$$

with internal stability.

Proof. The proof of the proposition follows standard arguments by noting that the error variable dynamic takes the form

$$\dot{\tilde{x}} = J(\alpha_2)\nabla H(\tilde{x}) + G(\tilde{x})\alpha_1(\tilde{D}, \tilde{f}_s) \tag{16}$$

where $\tilde{D} = D - D^\star$, $\tilde{f}_s = f_s - f_s^\star$ and

$$H(\tilde{x}) = \frac{1}{2}\tilde{x}^\top P \tilde{x}$$

Consider now the positive definite function

$$V(\tilde{x}, \zeta) = H(\tilde{x}) + \frac{1}{2}\zeta^\top K_I \zeta$$

whose time derivative along the trajectories of the error dynamic is given by

$$\dot{V}(\tilde{x}, \zeta) = \dot{H}(\tilde{x}) + \frac{1}{2}[\dot{\zeta}^\top K_I \zeta + \zeta^\top K_I \dot{\zeta}] \tag{17}$$

If the control structure (14) is considered, then it is obtained that $\dot{H}(\tilde{x}, \zeta) \leq 0$. Hence, the proof is concluded by the application of standard arguments.

□□□

IV. Numerical Evaluation

The usefulness of the proposed modeling methodology and the proposed control scheme are illustrated via numerical simulations carried out under the MATLAB/Simulink computational environment.

For this numerical evaluation there were considered ideal inductors and capacitors with values as reported in [23]. In addition, the following considerations were included:

- S_1 was implemented using the Simulink ideal switch considering $R_{on} = .0001\ \Omega$, $R_s = .00001\ \Omega$ and $C_s = \infty$.
- D_0 was implemented using the Simulink ideal diode model considering $V_f = 0.8V$, $R_{on} = .001\ \Omega$, $L_{on} = 0\ H$, $R_s = 500\ \Omega$ y $C_s = 250\ pF$.
- The signal α_1 was approximated considering $n = 5$.

Concerning the proposed model validation, Figure 6 shows the behavior of the resonant states x_1 and x_2 for both a discontinuous version of α_1 and its approximation. It is clear that with the selected number of the Taylor series components, the proposed model recovers the behavior of the discontinuous system close enough from a control point of view. Thus, this approximation was implemented to evaluate the control scheme performance.

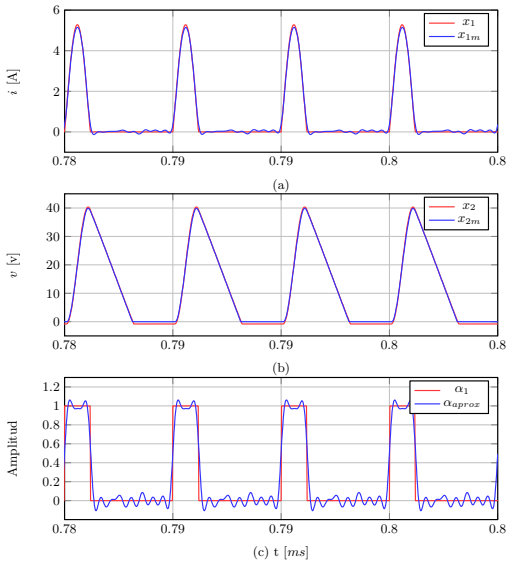

Fig. 6. Numerical validation of approximate model for $n = 5$.

With the aim to evaluate the usefulness of the proposed controller, the output voltage desired profile shown in Figure 7 (d) was considered. This behavior starts with a value of $16V$ to change its value to a lower value of $13V$. Additionally, when the voltage reference remains at this last value, a change in the load resistance (not considered by the theoretical design) is included. For this evaluation it was considered the values $K_p = 900$ and $K_I = 100$.

As can be noticed from the results presented in Figure 7, the performance of the closed-loop system is remarkable. This feature is illustrated, first, by noting that although the considered initial value for the output voltage was set to zero,

the convergence time was approximately $0.3ms$. Second, the transient response of the system under a load change exhibits a smooth behavior. Finally, even in presence of an unknown perturbation, the control objective is achieved.

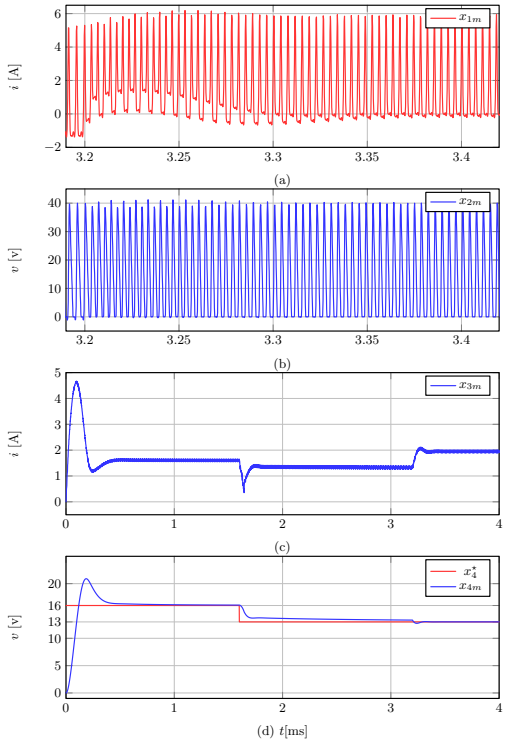

Fig. 7. Numerical evaluation of the passive PI controller.

V. Concluding Remarks

In this paper the modeling and control of QRBC is approached. Concerning the modeling objective, a novel PCH representation was introduced. In addition that its validity was illustrated in a numerical setting, its usefulness was exhibited to identify structural properties of the converter that are usually lost under classical representations like the widely used GSSA model. Regarding the proposed controller, it was shown that the PCH structure of the proposed model can be exploited to implement well-known PBC schemes for which, in addition to formally prove its stability properties, high performance responses are achieved.

References

[1] Biao Zhao, Qiang Song, Wenhua Liu, and Yandong Sun. Overview of dual-active-bridge isolated bidirectional dc–dc converter for high-frequency-link power-conversion system. *IEEE Transactions on power electronics*, 29(8):4091–4106, 2013.

[2] Yueshi Guan, Carlo Cecati, J Marcos Alonso, and Zhe Zhang. Review of high-frequency high-voltage-conversion-ratio dc–dc converters. *IEEE Journal of Emerging and Selected Topics in Industrial Electronics*, 2(4):374–389, 2021.

[3] Hadi Tarzamni, Homayon Soltani Gohari, Mehran Sabahi, and Jorma Kyyrä. Non-isolated high step-up dc-dc converters: comparative review and metrics applicability. *IEEE Transactions on Power Electronics*, 2023.

[4] Oscar Miguel Rodríguez-Benítez, Juan Antonio Aqui-Tapia, Isaac Ortega-Velázquez, and Gerardo Espinosa-Pérez. Current source topologies for photovoltaic applications: An overview. *Electronics*, 11(18):2953, 2022.

[5] Juan M Carrasco, Eduardo Galván, Gerardo Escobar Valderrama, Romeo Ortega, and Aleksandar M Stankovic. Analysis and experimentation of nonlinear adaptive controllers for the series resonant converter. *IEEE Transactions on power Electronics*, 15(3):536–544, 2000.

[6] Zhijian Fang, Junhua Wang, Shanxu Duan, Kaipei Liu, and Tao Cai. Control of an llc resonant converter using load feedback linearization. *IEEE Transactions on Power Electronics*, 33(1):887–898, 2017.

[7] Fouad Giri, O El Maguiri, H El Fadil, and Fatima Zara Chaoui. Nonlinear adaptive output feedback control of series resonant dc–dc converters. *Control engineering practice*, 19(10):1238–1251, 2011.

[8] Eduardo Sebastián, Eduardo Montijano, Estanis Oyarbide, Carlos Bernal, and Rubén Gálvez. Nonlinear implementable control of a dual active bridge series resonant converter. *IEEE Transactions on Industrial Electronics*, 69(5):5111–5121, 2021.

[9] Romeo Ortega, Antonio Loria, Per Johan Nicklasson, Hebertt Sira-Ramirez, Romeo Ortega, Antonio Loría, Per Johan Nicklasson, and Hebertt Sira-Ramírez. *Euler-Lagrange systems*. Springer, 1998.

[10] Romeo Ortega, Arjan Van Der Schaft, Fernando Castanos, and Alessandro Astolfi. Control by interconnection and standard passivity-based control of port-hamiltonian systems. *IEEE Transactions on Automatic control*, 53(11):2527–2542, 2008.

[11] Romeo Ortega, José Guadalupe Romero, Pablo Borja, and Alejandro Donaire. *PID passivity-based control of nonlinear systems with applications*. John Wiley & Sons, 2021.

[12] Harini Sampath, Chellammal Nallaperumal, and Md Jahangir Hossain. Quasi-resonant converter for electric vehicle charging applications: Analysis, design, and markov model use for reliability estimation. *Energies*, 17(4):815, 2024.

[13] Hans Wouters and Wilmar Martinez. Bidirectional on-board chargers for electric vehicles: State-of-the-art and future trends. *IEEE Transactions on Power Electronics*, 2023.

[14] Xiao Long and Dongdong Chen. Small signal modeling of llc converter with led load and quasi-resonant controller based active ripple rejection. *Energies*, 16(9):3773, 2023.

[15] Mojtaba Forouzesh, Yam P Siwakoti, Saman A Gorji, Frede Blaabjerg, and Brad Lehman. Step-up dc–dc converters: a comprehensive review of voltage-boosting techniques, topologies, and applications. *IEEE transactions on power electronics*, 32(12):9143–9178, 2017.

[16] Giordano Luigi Schiavon, Eloi Agostini Jr, and Claudinor Bitencourt Nascimento. Quasi-resonant single-switch high-voltage-gain dc-dc converter with coupled inductor and voltage multiplier cell. *Energies*, 16(9):3874, 2023.

[17] Ilse Cervantes, David García, and Daniel Noriega. Linear multiloop control of quasi-resonant converters. *IEEE Transactions on Power Electronics*, 18(5):1194–1201, 2003.

[18] Kwang-Hwa Liu, Ramesh Oruganti, and Fred CY Lee. Quasi-resonant converters-topologies and characteristics. *IEEE Transactions on Power electronics*, (1):62–71, 1987.

[19] Aleksandar M Stankovic, David J Perreault, and Kenji Sato. Synthesis of dissipative nonlinear controllers for series resonant dc/dc converters. *IEEE Transactions on Power Electronics*, 14(4):673–682, 1999.

[20] XF Shi and CY Chan. A passivity approach to controller design for quasi-resonant converters. *Automatica*, 38(10):1727–1734, 2002.

[21] Mostafa Ali Ayubirad, Simin Amiri Siavoshani, and Mohammad Javad Yazdanpanah. A robust passivity based control strategy for quasi-resonant converters. *IET Power Electronics*, 14(7):1360–1370, 2021.

[22] Oscar Miguel Rodríguez-Benítez, Isaac Ortega-Velázquez, Agustín Sánchez-Contreras, and Gerardo Espinosa-Pérez. Modified pi controller for robustness improvement of quasi-resonant converters. *Processes*, 12(8):1762, 2024.

[23] A Rameshkumar and S Arumugam. Pi control of quasi-resonant buck converter. In *International Conference on Advances in Information Technology and Mobile Communication*, pages 477–485. Springer, 2012.